LA-UR- 96-1638

CONF-9606208--2

Title: PROPERTIES OF PLASMA RADIATION DIAGNOSTICS

Author(s): G. C. IDZOREK, P-22
H. Oona, DX-3

Submitted to: 11th topical conference on high temperature plasma diagnostics

PROPERTIES OF PLASMA RADIATION DIAGNOSTICS

G. C. Idzorek, H. Oona

ms #D410, Los Alamos National Laboratory, Los Alamos, New Mexico 87545

A number of diagnostics utilizing the radiation emitted from high-temperature plasmas have been developed at Los Alamos. Photoemissive x-ray diodes with photon energy bandpass filters provide time resolved rough spectral data from about 6 eV to >10 keV photon energy. Filtered silicon photodiodes can be used down to 1 eV and offer the advantages of nominally flat response and ability to operate in poor vacuum conditions. Both types of diodes will provide a rough time resolved spectrum and both are relatively inexpensive, reliable, and passive (i.e. no synchronization problems). For higher energy resolution bent crystal spectrographs are used in the x-ray region. With the addition of streak cameras or gated microchannel plates these systems provide data with high energy and high time resolution. To measure the total energy output a thin foil bolometer is used that measures the change in foil resistance as it is heated by the plasma radiation. Information on the physical location of the plasma is provided by a suite of visible framing cameras and x-ray pinhole cameras. By combining these diagnostics into a complementary set good diagnostic information can be guaranteed on any plasma experiment.

DISCLAIMER

X-RAY DIODES

Historically, photoemissive x-ray diodes (XRD's) have been used as soft x-ray detectors[1]. For a given metal photocathode in a parallel plate geometry the electrical limitations on signal output are the detector response time and maximum detector output current.

Maximum linear output current is limited by the electron space-charge distortion of the electric field between the anode and cathode of the detector. The space-charge limit can be calculated by solving Poisson's equation. Ignoring the initial electron velocities, assuming uniform illumination, and setting appropriate boundary conditions the solution[2-3] is:

$$I_{sp} = 2.33 \times 10^{-6} \frac{A V^{\frac{3}{2}}}{d^2} \text{ amperes}$$

Where I_{sp} is space-charge current limit, **A** is the detector area (m^2), **d** is the distance from cathode to anode (m), and **V** is the potential between anode and cathode (volts).

The time response of the detector is determined by the electron transit time from cathode to anode and the electrical time constant of the detector system. The rise time of the detector is then[4]:

$$t_r = 3.4 \times 10^{-6} \frac{d}{\sqrt{V}} \text{ seconds}$$

and the decay time is given by[4]:

$$t_d = 8.05 \times 10^{-12} \frac{R A}{d} \text{ seconds}$$

where **A**, **d**, and **V** are defined as before and **R** is the characteristic impedance of the signal line in ohms. For our pulsed power experiments we generally use a compact inexpensive detector designated the XRD-96 which consists of a 1 cm diameter aluminum photocathode biased at -1000 volts spaced 0.13 cm from an anode screen assembled on a vacuum-tight type TNC coaxial connector. Threaded onto the TNC is an aluminum barrel which holds the cathode, anode, and x-ray filters. The XRD-96 was designed as an inexpensive throw-away detector for our pulsed power experiments some of which are explosively driven and physically destroy the detectors and all of which blast debris at the detector assembly. The cathodes were machined from standard 1100 series aluminum and calibrated at our x-ray synchrotron facility at the National Synchrotron Light Source (NSLS), Brookhaven National Laboratory

on Long Island, New York[5]. Even when carefully prepared the cathode surface will show signs of carbon contamination (see Fig. 1). Once used the cathodes are often visibly contaminated and we have seen the response shift by factors of 2-3. Our experience has shown a cathode to cathode response variation of about 15% within a given batch of new aluminum cathodes. By discarding the detector after use we are not required to protect the XRD-96 with massive debris shields, fast-closing valves, fast bias voltage dump electronics, etc. and their associated high costs. This allows us to use large numbers of detectors at any many locations in our experiments. Being a photoemissive detector very small amounts of surface contamination can dramatically change the response of a photocathode since the typical range of photoelectrons can be measured in tens of angstroms. This extreme contamination sensitivity led us explore alternative detector technologies.

SILICON PHOTODIODES

Recent advances in fabrication technique have made the silicon photodiode detector attractive for soft x-ray experiments. Unlike older silicon photodiodes the vacuum ultra-violet detectors made by International Radiation Detectors[6] (IRD) are fabricated without a dead layer and a passivating layer only 60 angstroms thick. These features allow the new silicon photodiodes to be used at photon energies well below 100 eV. Other advantages of silicon photodiodes include low bias voltage (0 - 50 volts), insensitivity to surface contamination, long term stability, nominally flat response, fast rise time, ability to use very thin x-ray filters deposited directly onto the diode surface, and small size. These features have lead the National Institute of Standards and Technology (NIST formerly NBS) to the adoption of the IRD detectors as secondary standards for soft x-ray work.

We are currently using our beamlines at the NSLS to characterize the IRD type HS-1 detectors between 30 eV and 10 keV x-ray energy. In addition a visible light monochromator provides calibration data from 1 to 4.5 eV. Our visible measurements have confirmed the manufacturers claim of less 5% response variation between diodes and preliminary analysis of x-ray measurements also appears in agreement. Measured response values overlaid with a calculated response are shown in Fig. 2. The deviation from a nominally flat response in the visible and above 700 eV is due to our usage of the HS-1

diode without a limiting pinhole. The pinhole was not used in our detector designs due to the expense and difficulty of aligning multiple pinholes on our 7-element detector array. The HS-1 is fabricated with a 0.05 mm^2 "sensitive area" centered on a 1 mm^2 silicon chip. The sensitive area is passivated with a 60 angstrom SiO_2 window while the outer regions have about 8000 angstroms of SiO_2 for a protective layer. The response increases are due to visible light transmission through the transparent SiO_2 and x-ray transmission at the higher energies. This transmission increases the effective area of the detector causing an increase in response.

Electrical limitations of silicon photodiodes are determined by the silicon doping, depletion depth, and diffusion geometry. These parameters vary between manufacturers and some such as depletion depth change as a function of applied bias voltage. Rarely does one have adequate information or a sophisticated enough model to correctly calculate the electrical limitations. Measurements using a fast pulsed laser (45 ps fwhm, 54 mW, 850 nm wavelength) show the HS-1 to have about a 100 ps risetime and a 800 ps fall-time. We are in the process of using a high power ruby laser to measure the linearity and saturation limits of the HS-1 as a function of applied bias voltage.

CURVED CRYSTAL SPECTROMETER

The dispersion of a convex curved crystal spectrometer is a function of both crystal spacing and curvature. The curvature makes it possible to have a large dispersion with a small acceptance angle and therefore an increased spectral range for a given spectrometer. A geometrical relationship for dispersion is shown in Fig. 3. and this is modified by the Bragg condition $n\lambda=2d \sin \gamma$. Here λ is the wavelength in angstroms; d the lattice spacing; and γ the Bragg angle. The incident x-rays are at an angle γ relative to the normal of the crystal as shown in the figure. We have used these types of spectrometers to study x-rays in the range from 200 eV to 30 keV. They are very efficient but are only of moderate resolution but are convenient for doing survey spectrum of plasmas produced in pulse power and laser fusion experiments. For very soft x-rays (180-300 eV) we have used pseudo-crystals of lead stearate and lead melissate and for higher energies, crystals of KAP and lithium fluorite. In Fig. 4. we show a sample spectrum from a

laboratory test. The bright lines are copper Kα and Kβ, we also see a distinct continuum and lines from other contaminants.

Dispersed x-rays are recorded either on film or electronic cameras. For time integrated spectrum film is an ideal recording medium. Time resolved spectra requires the more sensitive and sophisticated electronic streak cameras. These are coupled to experimental areas by fused silica fibers to transfer visible light produced by x-ray scintillators. Fig. 5. shows a time resolved spectrum of a plasma generated by foil imploded using explosively driven generators. The signals generated at the scintillator were transmitted over 30 m of fiber to a streak camera in a bunker. Due to the finite size of fibers the spectral resolution is not optimal and actual spectral lines could be lost in spaces between the fibers. In this experiment fifty fibers were used with the spacing equal to three times the size of the active fiber. Future experiments will use a combination of fibers and silicon photodiodes for detectors. The x-ray photodiodes will provide an absolute measurement of x-ray intensity without the calibration difficulties associated with x-ray to visible conversion, visible coupling losses, camera losses, and film calibration.

BOLOMETERS

A bolometer[7] consists of a thin metallic foil that is vapor deposited on a fused silica substrate. The foil resistance increases when it absorbs incident radiation energy. Our bolometers use either one micron thick nickel or aluminum and have a usable energy range of 10^{-5} - 10^{-1} J/cm^2. Filters are used to select the photon energy range of the measured x-rays. Fig. 6. shows a schematic of our four channel bolometer system and the related equations. The foils are 2 mm by 12 mm and are separated by 4 mm. We have used these to measure radiation fluence in cylindrical foil implosions in pulsed power experiments. Fig. 7. shows data from two unfiltered channels an one filtered (aluminized Kimfoil) channel of a typical experiment. Power measured from two adjacent channels are within the 7 % accuracy of our measurements. The filtered channel shows harder x-rays appearing later in time.

In some cases the calculated and measured bolometer power pulse agree well. On one experiment we measured 240 kJ total fluence with unfiltered bolometers, 300 kJ with XRD's, and calculated 250 kJ. On another experiment bolometers measured 375 kJ and XRD's that viewed the

source on the directly opposite side measured 350 kJ of total radiation. However, another set of XRD's located at a right angle to these measurements gave a total radiation of 640 kJ. The large observed differences are due to the large instabilities produced and the foil material that appears between the detector and source that filter the x-ray radiation.

IMAGING

Evidence of this is shown in high speed pictures taken with a visible framing camera and stripline microchannel plate x-ray cameras. We observe in Fig. 8. that images taken with visible photons and those taken with x-ray photons are virtually identical. These suggest that the x-ray emitting areas are the same as that for visible images and that the radiating region is large. A sequence of just visible images shows the implosion area can get totally blocked by material.. We see that material 'flaps' appear at the top and bottom edges of the electrode and this material grows and obscures the central radiation area. We believe that the large perturbations and the 'flaps' are responsible for the large observed x-ray variation in our detectors.

ACKNOWLEDGMENTS

We wish to thank our many colleagues at Los Alamos, from Bechtel Nevada our calibration team stationed at the NSLS and the detector fabrication team at Las Vegas, Nevada. This work was supported under DOE contract W-7405-ENG-36.

[1] R. H. Day, R. H., P. Lee, E. B. Saloman and D. J. Nagel, J. Appl. Phys. **52**, 6965 (1981).

[2] I. G. Herrmann, *The Oxide-Coated Cathode Vol. 2*, (Chapman & Hall Ltd., London, 1951), Chap. 1.

[3] L. R. Koller, *The Physics of Electron Tubes*, (McGraw-Hill Book Company Inc., New York and London, 1937), Chap. 8.

[4] R. H. Day, R. H., P. Lee, E. B. Saloman and D. J. Nagel, Los Alamos Scientific Laboratory report no. LA-7941-MS, 1981.

[5] R. J. Bartlett, R. J., W. J. Trela, F. D. Michaud, S. H. Southworth, R. Rothe, and R. W. Alkire, in *X-Ray Calibration: Techniques, Sources, and Detectors*, R. B. Hoover, Editor, proc. SPIE 689, 200 (1986).

[6] K. W. Wenzel, C. K. Li, D. A. Pappas and R. Korde,IEEE Trans. Nuc. Sci. **41**, 979 (1994).

[7] J. H. Degnan, Rev. Sci. Instrum. **50**, 1223 (1979).

FIG. 1. Measured x-ray response of machined series 1100 aluminum photocathodes. Note the jump at the C-K absorption edge (284 eV) due to surface contamination.

FIG. 2. Measured photon response of IRD type HS-1 silicon photodiode. Thin line is calculated response and thick line is measured response. Response units are in terms of intensity rather than power due to changing sensitive area as function of energy.

FIG. 3 Crystal spectrograph, dispersion geometry and generic equations. For given crystal with lattice spacing d, the Bragg condition requires that $\gamma = \sin^{-1}(n\lambda/2d)$.

FIG. 4 Spectrograph image of copper x-ray source. The bright spectral lines are Cu-Kα at 8.04 keV (left) and Cu-Kβ at 8.90 keV some continuum is also apparent.

FIG 5. Time resolved streak spectrum taken of plasma produced in a pulse power experiment. A scintillator was used to convert x rays to visible light and light was transported over optical fibers to a streak camera. The resolution is limited by fiber size and spacing

FIG. 6 The four channel thin foil bolometer. The equations shown are used to calculate the fluence. Filters are used to select the photon energy range of the measured x-rays.

FIG. 7 Data from the four channel bolometer. Power measured from adjacent channels of the bolometer. The two top curves are from two unfiltered adjacent channels and measure soft x-rays. The bottom curve is a filtered channel measure x-rays above 300 eV.

FIG. 8 Comparison of aluminum filtered x-ray image (top) and a visible framing image (bottom). Similarities suggest the same emitting regions for both x rays and visible light. The large instabilities

suggest that colder material masks the hot implosion region thereby modifying the observed x-ray spectrum.

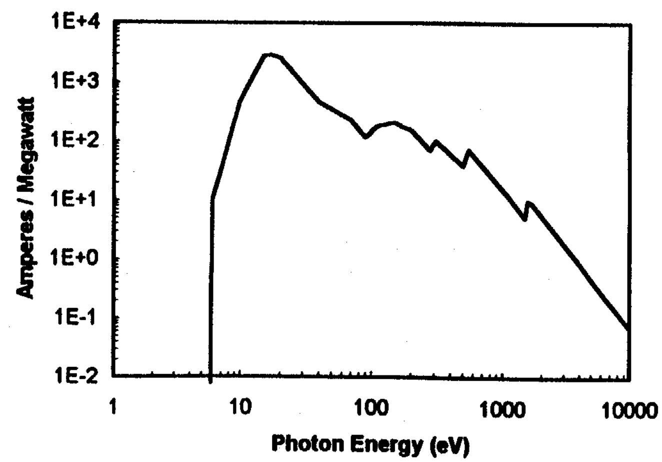
1E+4
1E+3
1E+2
1E+1
1E+0
1E-1
1E-2
Amperes / Megawatt
1
10
100
1000
10000
Photon Energy (eV)

FIG. 1 [illegible] et al.

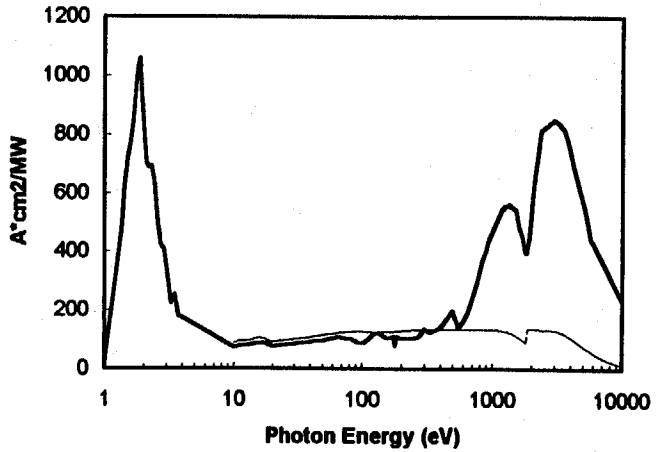
1200
1000
800
600
400
200
0
A*cm2/MW
1
10
100
1000
10000
Photon Energy (eV)

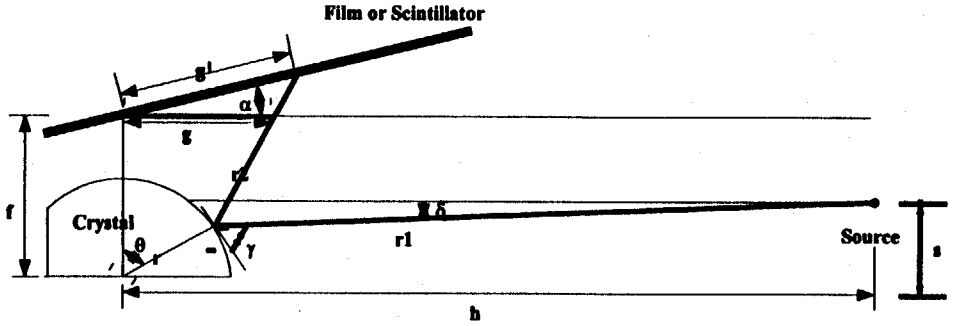

$\delta = \tan^{-1}((s - r\cos\theta)/(h - r\sin\theta))$

$\gamma = \theta + \delta$

$g = r\sin\theta + (r\cos\theta - \phi)/\tan(2\theta + \delta)$

$g' = g(\sin(2\theta + \delta)/\sin(2\theta + \delta + \alpha))$

$r_1 = (f - r\sin\theta)/r\sin(2\theta + \delta) + g((\sin\alpha/\sin(2\theta + \delta + \alpha))$

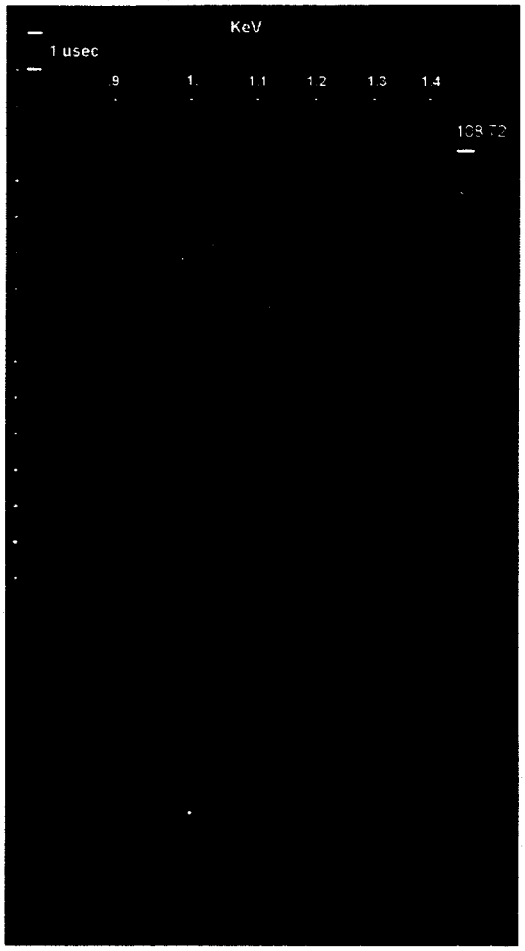
KeV
1 usec
.9
1.
1.1
1.2
1.3
1.4

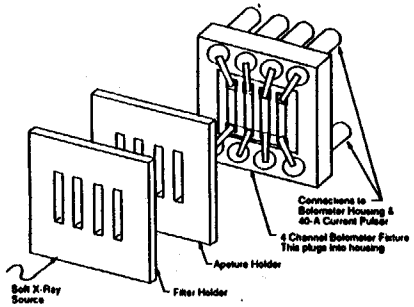

BOLOMETER SENSITIVITY

$$F_R=(\Delta V/I)*(1/(\Delta\rho/\Delta\varepsilon)*\upsilon*(W/L)*X^2$$

WHERE :

ΔV=CHANGE IN VOLTAGE DUE TO RESISTANCE CHANGE
F_R=RADIATION FLUENCE
I= CURRENT IN BOLOMETER FOIL
$\Delta\rho/\Delta\varepsilon$=RESISTIVITY CHANGE WITH SPECIFIC ENERGY
υ=BOLOMETER FOIL DENSITY
L=RADIATED LENGTH OF FOIL
W=RADIATED WIDTH OF FOIL
X=FOIL THICKNESS

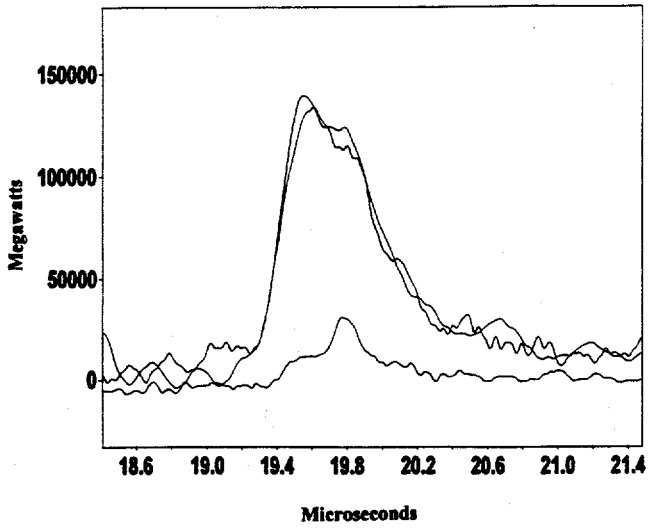

FIG 7 IDZOREK et al REV SCI INST